

# Kelvin-Helmholtz Instability in a Weakly Ionized Medium

C. Watson<sup>1</sup>, E.G. Zweibel<sup>1,2</sup>, F. Heitsch<sup>1,3</sup>, E. Churchwell<sup>1</sup>

## ABSTRACT

Ambient interstellar material may become entrained in outflows from massive stars as a result of shear flow instabilities. We study the linear theory of the Kelvin - Helmholtz instability, the simplest example of shear flow instability, in a partially ionized medium. We model the interaction as a two fluid system (charged and neutral) in a planar geometry. Our principal result is that for much of the relevant parameter space, neutrals and ions are sufficiently decoupled that the neutrals are unstable while the ions are held in place by the magnetic field. Thus, we predict that there should be a detectably narrower line profile in ionized species tracing the outflow compared with neutral species since ionized species are not participating in the turbulent interface with the ambient ISM. Since the magnetic field is frozen to the plasma, it is not tangled by the turbulence in the boundary layer.

## 1. Introduction

In the process of forming, massive ( $> 10 M_{\odot}$ ) stars produce massive bipolar outflows. In contrast to outflows from low-mass proto-stars, outflows from massive stars frequently have more mass than their presumed driving proto-star (Churchwell 1997). The canonical explanation for the origin of the mass is that a less massive jet originating from either the accretion disk or protostar sweeps up and entrains ambient interstellar material. This model can potentially explain both the large masses and poor collimation of massive outflows. It may also explain how low-mass outflows become less collimated as they age (Bachiller and Tafalla, 1998). Churchwell (1997) argued that mechanical entrainment, through e.g. bow-shocks, could not simultaneously explain both the large mass and young age of massive outflows.

---

<sup>1</sup>Univ. of Wisconsin - Madison, Dept. of Astronomy, 475 N. Charter St., Madison, WI 53716

<sup>2</sup>Center for Magnetic Self Organization in Laboratory & Astrophysical Plasmas, Univ. of Wisconsin, Madison

<sup>3</sup>Institute for Astronomy & Astrophysics, Scheinerstr. 1, 81679 Munich, Germany

Shear flow, or Kelvin-Helmholtz, instabilities at the interface between the jet and the ambient material are an alternative possible mechanism for entrainment. The instability amplifies ripples at the interface, culminating in the development of a turbulent boundary layer which can transfer momentum from the jet to the ambient medium. A magnetic field parallel to the flow tends to suppress the instability because magnetic tension opposes rippling. The result is that instability is only present if the velocity shear is greater than the Alfvén velocity (Chandrasekhar, 1961).

The nonlinear development of the Kelvin-Helmholtz instability is strongly influenced by the magnetic field (Malagoli et al., 1996 & Jones et al., 1997). The numerical simulations performed by these authors show that the vortices created by the instability wind up the field until it reaches the Ohmic scale. Windup transfers energy to small scales, while Ohmic dissipation heats the layer. These effects are absent in the field-free case.

In the following study, we investigate the Kelvin-Helmholtz instability in the linear, partially ionized regime to determine its possible contribution to entrainment in massive bipolar outflows. This problem cannot be analyzed in the hydrodynamic regime because the neutral Alfvén velocity ( $v_A = \frac{B}{\sqrt{4\pi\rho_n}}$ ) is sometimes larger than the flow speed, indicating that the magnetic field can be strong enough to affect the dynamics. On the other hand, the pure magnetohydrodynamic (MHD) regime is inappropriate because at sufficiently short wavelengths, Alfvén waves propagate nearly independently of the neutrals.

In §2 we describe a model that we believe is appropriate for massive outflows driven by massive protostars. In §3 we discuss the numerically-derived solutions to the dimensionless dispersion equation and equivalent analytical solutions to simplified versions of the dispersion equation. We demonstrate that there is a new instability, unique to the partially ionized regime, which results from ion-neutral slip. In §4, we discuss the observational implications of our results, concentrating on the physical environment of the interaction zone between a bipolar outflow and the ambient interstellar material (ISM). §5 is a critical summary of the paper.

## 2. Model Description

We model the interaction zone between a high speed jet and the ambient ISM by a slab geometry with a flow along the  $x$ -axis. The interface between the two fluids is the  $x - y$  plane. The density is everywhere uniform, and the velocity is uniform except at  $z = 0$ , where it has a step. We assume the flow velocity  $U$  decreases with increasing  $z$ . The magnetic field is uniform and aligned with the flow, which maximizes its stabilizing effect in the  $x$ -direction.

In this model, the equilibrium flow has zero vorticity except on the plane  $z = 0$ , where the vorticity is infinite. For our choice of coordinates and velocity profile, the total vorticity integrated across the sheet is  $-2U\hat{y}$ .

The mechanism of the Kelvin-Helmholtz instability is explained in Batchelor (1967). Suppose the interface is perturbed by a small amplitude ripple, as shown, in the center of mass frame, in Figure 1. Denote the vertical displacement of the vortex sheet by  $\eta$ . In general, the vorticity perturbation is out of phase with  $\eta$ . If it can be arranged that the vorticity has the distribution shown by the dashed line, then the equilibrium flow sweeps negative vorticity toward point  $P$  on both sides of the interface. The effect is as if an extra eddy, rotating counterclockwise as sketched in the Figure, were added to the flow. The centrifugal force associated with the eddy pushes the interface between  $P$  and  $Q$  outward, resulting in the growth of  $\eta$  with time. If the vorticity perturbation were shifted in phase by  $\pi$  with respect to the dashed line,  $\eta$  would shrink. As explained here, the instability mechanism requires advection of vorticity by the bulk flow in opposite directions above and below the interface. It is always possible to choose a reference frame in which this is the case, provided that the velocity profile has a jump.

A magnetic field parallel to the flow exerts a tension force when bent. The tension force is stabilizing, and the criterion that it dominates hydrodynamic forces is roughly that the magnetic energy exceeds the kinetic energy of relative motion, or, equivalently, that the Alfvén speed for the bulk medium exceed the flow speed.

The basic mechanism of instability is unaffected by partial ionization. In the weakly ionized medium of interest here, the plasma component tends to be stable, because its low density implies low kinetic energy. The neutral component, on the other hand, is intrinsically unstable because it is not directly acted upon by magnetic forces. Friction between the ions and neutrals allows magnetic forces to act on the neutrals. As we will see, however, no matter how large the magnetic field is, it cannot stabilize the neutrals completely.

In the present discussion, we follow the analysis of Chandrasekhar (1961) but consider two fluids, charged and neutral, coupled by elastic collisions<sup>1</sup>. We assume the medium is incompressible ( $\nabla \cdot \mathbf{v}_{i,n} = 0$ ). Our problem is described by the neutral and ion momentum equations and the magnetic induction equation:

$$\rho_n \partial_t \mathbf{v}_n + \rho_n \mathbf{v}_n \cdot \nabla \mathbf{v}_n = -\nabla P_n - \rho_n \nu_{ni} (\mathbf{v}_n - \mathbf{v}_i) \quad (1)$$

---

<sup>1</sup>We ignore coupling by ionization and recombination, since these processes are slow in comparison to elastic processes.

$$\rho_i \partial_t \mathbf{v}_i + \rho_i \mathbf{v}_i \cdot \nabla \mathbf{v}_i = -\nabla P_i - \rho_n \nu_{ni} (\mathbf{v}_i - \mathbf{v}_n) + \frac{1}{4\pi} (\nabla \times \mathbf{B}) \times \mathbf{B} \quad (2)$$

$$\partial_t \mathbf{B} = \nabla \times (\mathbf{v}_i \times \mathbf{B}), \quad (3)$$

where

$$\nu_{ni} \equiv \gamma \rho_i \quad (4)$$

is the neutral-ion collision frequency, and

$$\gamma \equiv \frac{\langle \sigma v \rangle}{m_i + m_n} \quad (5)$$

is the collision rate coefficient per unit mass.

The system consisting of two constant density, constant pressure regions of uniform flow aligned with a uniform magnetic field is clearly a steady state solution of eqns. (1 - 3). We now consider small perturbations of the flow. We assume these perturbations are independent of  $y$ . According to Squires' Theorem (Drazin & Reid 1981) and its extension to MHD (Hughes & Tobias 2001), in the absence of viscosity and resistivity these are the fastest growing perturbations. Since the magnetic field enters the problem only through the tension force, which is independent of the structure in  $y$ , ion-neutral friction should not affect this result. We expand the momentum and induction equations to first order in a small parameter  $\epsilon$ , writing

$$v_x \equiv u = U + \epsilon u \quad (6)$$

$$v_y \equiv w = \epsilon w \quad (7)$$

$$B_x = B + \epsilon b_x \quad (8)$$

$$B_z = \epsilon b_z. \quad (9)$$

We assume all perturbed quantities  $q$  take the form

$$q = q_0 e^{i(\omega t + k_x x) + \kappa z}, \quad (10)$$

where  $q_0$  is a constant amplitude. Linearizing in  $\epsilon$  gives

$$\rho_n (\partial_t + U \partial_x) u_n = -\partial_x P_n + \rho_n \nu_{ni} (u_i - u_n) \quad (11)$$

$$\rho_n (\partial_t + U \partial_x) w_n = -\partial_x P_n + \rho_n \nu_{ni} (w_i - w_n) \quad (12)$$

$$\rho_i (\partial_t + U \partial_x) u_i = -\partial_x P_i + \rho_n \nu_{ni} (u_n - u_i) \quad (13)$$

$$\rho_i (\partial_t + U \partial_x) w_i = -\partial_x P_i + \rho_n \nu_{ni} (w_n - w_i) + \frac{B}{4\pi} (\partial_x b_z - \partial_z b_x) \quad (14)$$

$$(\partial_t + U \partial_x) b_x = B \partial_x u_i \quad (15)$$

$$(\partial_t + U \partial_x) b_z = B \partial_x w_i, \quad (16)$$

which correspond to the equations (180-183) in Ch. 12 of Chandrasekhar (p. 508-9). Eliminating  $B$  in equation (14) using equations (15) and (16), constructing the  $\hat{z}$  component of the curl of the momentum equations, and applying  $\nabla \cdot \mathbf{v}_{i,n} \equiv 0$ , we obtain

$$\left( \rho_i(\omega + Uk_x) - \frac{B^2 k_x^2}{4\pi(\omega + Uk_x)} \right) (\partial_z^2 - k_x^2) w_i = i\rho_n \nu_{ni} (\partial_z^2 - k_x^2) (w_i - w_n) \quad (17)$$

$$\rho_n(\omega + Uk_x) (\partial_z^2 - k_x^2) w_n = i\rho_n \nu_{ni} (\partial_z^2 - k_x^2) (w_n - w_i) \quad (18)$$

These relations hold in each region, but not at the interface, where the velocity is not analytic. Thus, to derive the dispersion relation, we must integrate each equation over an infinitesimal region surrounding  $z = 0$  and use standard Gaussian pillbox arguments. Denoting the jumps in quantities by  $\Delta\{\}$ , we get

$$\Delta\{\rho_i(\omega + Uk_x)\partial_z w_i\} = i\Delta\{\rho_n \nu_{ni} \partial_z (w_i - w_n)\} + \frac{B^2 k_x^2}{4\pi} \Delta\left\{\frac{\partial_z w_i}{\omega + Uk_x}\right\} \quad (19)$$

$$\Delta\{\rho_n(\omega + Uk_x)\partial_z w_n\} = i\Delta\{\rho_n \nu_{ni} \partial_z (w_n - w_i)\}. \quad (20)$$

We write the ion and neutral velocity amplitudes in the form

$$w_{i1} = \mathcal{A}(\omega + U_1 k) e^{kz} \quad z < 0 \quad (21)$$

$$w_{i2} = \mathcal{A}(\omega + U_2 k) e^{-kz} \quad z > 0 \quad (22)$$

$$w_{n1} = \mathcal{B}(\omega + U_1 k) e^{kz} \quad z < 0 \quad (23)$$

$$w_{n2} = \mathcal{B}(\omega + U_2 k) e^{-kz} \quad z > 0, \quad (24)$$

where the subscripts 1 and 2 refer to the jet and ambient medium, respectively. The forms of  $w_{i,n}$  are chosen such that the ion and neutral displacements are continuous across the interface, as must hold on physical grounds. Substituting these forms into equations (19) and (20), we solve for  $\mathcal{B}$ , the neutral velocity fluctuations, in terms of  $\mathcal{A}$ , the ion velocity fluctuations. The result is

$$\mathcal{B} = -i \frac{\rho_{n1} \nu_1 (\omega + U_1 k_x) + \rho_{n2} \nu_2 (\omega + U_2 k_x)}{\rho_{n1} (\omega + U_1 k_x) (\omega + U_1 k_x - i\nu_1) + \rho_{n2} (\omega + U_2 k_x) (\omega + U_2 k_x - i\nu_2)} \mathcal{A}. \quad (25)$$

We then use equations (21) and (25) in equation (19) to obtain the dispersion relation

$$\begin{aligned} \rho_{i1}(\omega + U_1 k)^2 + \rho_{i2}(\omega + U_2 k)^2 &= (\rho_{n1} \nu_1 (\omega + U_1 k) + \rho_{n2} \nu_2 (\omega + U_2 k)) \times \\ &\left( i - \frac{(\rho_{n1} \nu_1 (\omega + U_1 k) + \rho_{n2} \nu_2 (\omega + U_2 k))}{\rho_{n1} (\omega + U_1 k) (\omega + U_1 k - i\nu_1) + \rho_{n2} (\omega + U_2 k) (\omega + U_2 k - i\nu_2)} \right) + \\ &+ \frac{B^2 k^2}{2\pi} \end{aligned} \quad (26)$$

where  $\nu_{ni}$  has been abbreviated to  $\nu$  and  $k_x$  abbreviated to  $k$ .

We now assume that the jet and ambient medium have the same density, work in the center of momentum frame so that

$$\begin{aligned} U_1 &= -U_2 = U \\ \rho_{n1} &= \rho_{n2} = \rho_n \\ \rho_{i1} &= \rho_{i2} = \rho_i, \end{aligned} \tag{27}$$

and nondimensionalize the problem as follows:

$$\begin{aligned} m &\equiv \frac{\rho_n}{\rho_i} \\ x &\equiv \frac{\omega}{\nu} \\ h &\equiv \frac{Uk}{\nu} \\ a &\equiv \frac{\sqrt{m}Bk}{\nu\sqrt{4\pi\rho_n}} = \frac{kv_{Ai}}{\nu}, \end{aligned} \tag{28}$$

where the ion Alfvén speed  $v_{Ai}$  is defined as  $\frac{B}{\sqrt{4\pi\rho_i}}$ . The variables  $x$ ,  $h$  and  $a$  represent the perturbation frequency, flow speed and ion Alfvén speed, respectively.

Substituting equations (27) and (28) into equation (26) we obtain

$$x^4 - i(m+1)x^3 + (2h^2 - a^2)x^2 - i(mh^2 - a^2 + h^2)x + h^2(h^2 - a^2) = 0. \tag{29}$$

In all cases of interest,  $m \gg 1$  and  $a \gg h$ , which allows us to drop a few of the terms in equation (29). This leads to the somewhat more compact expression

$$x^4 - imx^3 - a^2x^2 - i(mh^2 - a^2)x - a^2h^2 = 0. \tag{30}$$

Equation (30) is the basis of our subsequent stability analysis. We will be looking for solutions for  $x$  which have a negative imaginary component, an indication of a growing instability.

### 3. Analysis of the Dispersion Relation

Equations (29) and (30) reduce, in special cases, to previously known results. These are discussed in §3.1. In §3.2 we present numerical and analytical solutions for the fastest growing modes. In §3.3 we discuss the physical nature of the instabilities.

### 3.1. Recovery of previously known results

If  $h \equiv 0$ , equation (30) reverts to the dispersion relation for Alfvén waves in a partially ionized medium (Kulsrud & Pearce 1969)

$$x(x^2 - a^2) - i\left(x^2 - \frac{a^2}{m}\right) = 0. \quad (31)$$

At sufficiently small wavenumber ( $k < \frac{2\nu_{ni}}{v_{An}}$ ;  $a < 2\sqrt{m}$ ) the wave speed is close to the neutral Alfvén velocity  $v_{An}$  because the neutral-ion collision timescale is less than the wave period and the ion and neutral species are closely coupled. We can derive this result from equation (31) by treating the second factor in parentheses as dominant. This leads to

$$x \approx \pm \frac{a}{\sqrt{m}} + i\frac{a^2}{2m}, \quad (32)$$

which is a weakly damped Alfvén wave propagating at speed  $v_{An}$ .

At sufficiently large wavenumber ( $k > \frac{\nu_{in}}{2v_{Ai}}$ ;  $a > m/2$ ), the wave period is shorter than the ion-neutral collision timescale. Thus, Alfvénic disturbances are able to propagate through the ions without disturbing the neutrals and propagate at the ion Alfvén velocity  $v_{Ai}$ . We can derive this result from equation (31) by treating the first factor in parentheses as dominant. This leads to

$$x \approx \pm a + i\frac{m}{2}, \quad (33)$$

which is a damped wave propagating at the ion Alfvén velocity. In the intermediate wavenumber regime ( $2\sqrt{m} < a < m/2$ ), waves cannot propagate because the ions are poorly coupled to neutrals and thus feel a strong drag.

The shear instability in a fully-neutral medium (or ionized but magnetic field free) is present at any velocity and has growth rate  $kU$  ( $\equiv h$  in our notation). In order to recover the hydrodynamic instability we must use equation (29) with  $a \equiv 0$ . The dispersion relation can then be written in the form

$$(x^2 + h^2) [x^2 - i(m+1)x + h^2] = 0. \quad (34)$$

The hydrodynamic instability is the root  $x = -ih$ .

On the other hand, a fully ionized medium with a magnetic field parallel to the shear flow is stabilized by magnetic tension if  $U < v_A$ . In order to recover the MHD instability, we set  $m \equiv 0$  in equation (29) and write the dispersion relation in the form

$$(x^2 + h^2 - a^2) (x^2 + h^2 - ix) = 0. \quad (35)$$

Note that the growth rates of both hydrodynamic and MHD instabilities increase linearly with wavenumber.

### 3.2. The most unstable roots

With §3.1 as background, we now turn to the shear instability in the partially ionized regime.

If there were no ion-neutral friction, the neutrals would always be unstable. The plasma would be stable if  $U < v_{Ai}$  ( $h < a$ ), which we assume to be the case. Since the growth rate of the hydrodynamic instability increases with  $k$ , there is a wavenumber above which friction with the ions cannot stabilize the perturbation. Therefore, we expect short wavelength perturbations to grow at the hydrodynamic rate in the neutral fluid, but to leave the plasma and magnetic field in place.

At longer wavelengths, there is time for ion-neutral friction to act. If  $v_A < U$  ( $a < h\sqrt{m}$ ), the magnetic field cannot be expected to stabilize the medium no matter how well the ions and neutrals are coupled. On the other hand, if  $U < v_A$ , we might expect that at sufficiently long wavelengths the coupling is good enough to completely stabilize the system. We will see, however, that this is never the case.

We carried out a parameter study of the roots of equation (30) as functions of  $a$  and  $h$  using the Mathematica software package (Wolfram 1999). Surprisingly, the roots are closely approximated by the analytical expressions given in Table 1 for the specified range of dimensionless parameters. In the results presented here, we focus on two sets of physical environments which we believe are illustrative of the range of conditions encountered in molecular outflows. The density of the ambient medium near massive protostars is a strong function of distance from the protostar. within radii of 100-1000 AU densities are  $\lesssim 10^5$   $\text{cm}^{-3}$ , further out where outflows can be easily resolved and structure studied densities of  $10^3$   $\text{cm}^{-3}$  are typical. In both examples, we take the molecular hydrogen density  $n(H_2)$  to be  $10^3$   $\text{cm}^{-3}$ , the relative flow speed  $2U$  to be 20  $\text{km s}^{-1}$ , and the ratio  $m$  of neutral to ionized mass density to be  $10^6$  (corresponding to an ionization fraction  $\sim 10^{-7}$  for an ion to neutral particle mass ratio  $\sim 10$ ). The collision frequency  $\nu$  is  $1.5 \times 10^{-13}$   $\text{s}^{-1}$  (we use the rate coefficient of Draine, Roberge, & Dalgarno (1983);  $\langle\sigma v\rangle = 1.5 \times 10^{-9}$   $\text{cm}^2 \text{s}^{-1}$ ). With the these values, the wavelength at which the hydrodynamic frequency  $kU$  matches the collision frequency ( $h = 1$ ) is about 1.3 pc. The only difference between the two cases is in the magnetic field strength, which we take to be 1  $mG$  (strong field case) and 1  $\mu G$  (weak field case). With these parameters,  $a/h = 4400$  and 4.4 in the strong and weak field cases,



respectively.

Since only growing modes will be dynamically important in the interface between a fast moving jet and the ambient ISM, we restrict our discussion to two solutions,  $-ih$  [and the variant  $-i(\frac{1}{2} - h)$ ] and  $-ih^2$ . Confirmation that these expressions closely approximate the numerically derived roots is shown in Figure 2. The numerically determined roots to the dispersion equation are shown as a function of wavelength; overplotted are the analytical approximations to the two growing modes. The wavelengths  $2\pi/k$  and growth times  $(Im(\omega))^{-1}$  are plotted in physical units for the two cases specified above.

The analytical solutions can be derived from the dispersion relation by dropping small terms. The dominant terms used to derive each solution are given in Table 1. For example, the first root listed,  $-ih$ , is the standard hydrodynamic instability derived from equation (34). From the dispersion relation, we can see that the terms  $\propto a^2$  ( $-a^2x^2$ ,  $ia^2x$ ,  $-a^2h^2$ ) are dominant in the high magnetic field regime. Of the  $a^2$  terms, the terms  $\propto h^2$ ,  $x^2$  dominate over the term  $\propto x$  because  $h > 1$ . In contrast, when  $h < 1$ , the terms  $\propto x$ ,  $h^2$  dominate, and the growing mode is  $-ih^2$ .

This second growing mode,  $-ih^2$ , is a new mode that arises only in a weakly ionized medium. It originates when  $h < 1$ , or equivalently  $kU < \nu$ . The neutrals feel a constant drag force, independent of position, caused by collisions with the stationary ions. The instability has an origin similar to the standard hydrodynamic instability explained in §2. The principal difference is that the neutral-ion collision time is shorter than the wave period. Thus, neutral material collides with ions (held stationary because of the magnetic field tension) frequently during each perturbation period, which slows the growth of small perturbations. This slowing of the growth is clearly visible in Figure 2 (bottom panel) where the growth time is longer for long wavelength (and long period) perturbations. The origin of this mode can be made more clear by assuming the ions are held strictly in place by the magnetic field and re-deriving the roots (see Appendix A). The break between the two growing modes occurs when  $h = 1$  or, equivalently,  $\frac{1}{Uk}$  (the wave period) =  $\frac{1}{\nu}$  (the neutral-ion collision timescale). See Figure 3 for physical parameters of this transition. Since this mode grows more slowly than the  $-ih$  mode, it is important only in the situation  $U < v_A$  (or  $\sqrt{mh} < a$ ), when the MHD mode is stable.

When  $\sqrt{mh} > a$  and  $h < 1$ ,  $-ih\sqrt{1 - a^2/mh^2}$  is a better approximation to the growth rate. This is the analog of eqn. (35) for a fully ionized medium. It is based on the limit of infinitely strong ion-neutral coupling.

### 3.3. Physical nature of the unstable modes

One of the main results of §3.2 is that the plasma and the neutrals can follow very different dynamics as the instability grows. Although the interface between the two regions of flow is the same for the plasma as for the neutrals in the equilibrium system, the displaced interfaces for the plasma and neutral species can differ, as can their velocities. The negligibly small inertia of the ions renders any differences irrelevant to the basic mechanism of instability, but they are important for the nonlinear outcome of the instability, and for its spectroscopic signatures.

On physical grounds, we expect large differences between  $v_i$  and  $v_n$  when ion - neutral coupling is weak ( $h > 1$ ) and magnetic forces are strong. Whether these differences persist at small  $h$  depends on the relative values of  $a/\sqrt{m}$  and  $h$ . If their ratio is less than unity the field is too weak to suppress instability even in the limit of infinitely strong ion-neutral coupling, and we expect  $v_i \sim v_n$ . If  $a/h\sqrt{m} > 1$  the instability acts on the neutrals but leaves the ions behind, and we expect large differences between  $v_i$  and  $v_n$  even at short wavelengths.

These expectations are borne out by analysis. According to equation (21), the amplitudes of the ion and neutral displacements are  $\mathcal{A}$  and  $\mathcal{B}$ , respectively. Their ratio follows from equation (25), which for the problem at hand can be written in dimensionless form using equations (28) as

$$\frac{\mathcal{B}}{\mathcal{A}} = \frac{-ix}{x^2 + h^2 - ix}. \quad (36)$$

The modulus of the relative amplitude is plotted as functions of wavelength in Figure 4 for the  $v_A > U$  and  $v_A < U$  cases, respectively. When the field is strong and  $h$  is large (short wavelength), the ions are held firmly in place and the instability is almost entirely in the neutrals, so  $|\mathcal{B}/\mathcal{A}|$  is large. The numerical results are well fit by the asymptotic formula  $|\mathcal{B}/\mathcal{A}| \sim a^2/mh \propto \lambda^{-1}$ . As  $h$  decreases the coupling improves, but the magnetic restoring force is still very large and the ion response never matches the neutrals. In this regime,  $|\mathcal{B}/\mathcal{A}| \sim a^2/mh^2$ . Recall (see Figure 2) that in this limit the instability is of the weak form  $x \sim -ih^2$ .

When the field is weak, magnetic forces are relatively unimportant. In this case,  $|\mathcal{B}/\mathcal{A}|$  is nearly unity over most of the range considered, although Figure 4 (bottom panel) shows a slight upturn at the shortest wavelengths, at which ion-neutral friction is relatively weak. The location of the upturn shows the expected scaling with  $B$ . For example, at  $\lambda = 280$ ,  $|\mathcal{B}/\mathcal{A}| \sim 1$  for  $B = 1\mu G$ , increasing to 25 if  $B = 10\mu G$  and 50 if  $B = 20\mu G$ . In all three cases, however,  $|\mathcal{B}/\mathcal{A}|$  drops to unity for  $h < 1$  ( $\lambda \sim 2.8 \times 10^6$  AU). Not until the field is

strong enough to stabilize the bulk medium  $B \sim 230\mu G$  does  $|\mathcal{B}/\mathcal{A}|$  exceed unity for  $h < 1$ .

In deriving both the numerical and asymptotic results in the cases where  $x \sim -ih$ , the  $x^2$  and  $h^2$  terms in the denominator of eqn. (36) nearly cancel. Thus, the right hand side of the equation (36) must be computed using roots to the exact dispersion relation (equation (29)).

The critical result from this analysis is that if  $B \gtrsim 10\mu G$  then at relevant length scales and timescales for bipolar outflows ( $l < 1000$  AU and  $\tau < 1000$  years), the fluctuations are primarily in the neutrals and not in the ions or magnetic field. In contrast to the MHD shear flow instabilities simulated by Jones et al. (1996) and Malagoli et al. (1996), the magnetic field cannot wind up and dissipate on small scales, and the instability is primarily hydrodynamic in character. We now turn to the observational implications of this conclusion.

## 4. Observational Implications

The calculations presented here do not permit quantitative predictions for observational signatures of the two instabilities for ambient ISM entrainment by massive bipolar outflows. We would need to develop numerical models with two fluid MHD that incorporate non-planar geometry and non-linear growth, and would need chemical models and radiative transfer calculations to predict the resulting spectra. Such an analysis is beyond the scope of this paper. However, several physical signatures should be robust, and may be observable.

### 4.1. Molecular Spectroscopy

As we showed in §3.3, unless  $B$  is less than about  $10\mu G$ , over most of the parameter space of interest only neutrals participate in the resulting turbulence. That is, only neutrals will have a velocity significantly different from either the outflow jet or the ambient ISM. For example, if outflow jets had uniform velocity emerging from the protostar, then the emission from ionized molecules should not be detectable at velocities different from the outflow velocity. This signature should be particularly distinctive if there are ion species that are present in only one of these media. Outflow jets probably have a range in velocity, however, which will make isolating a velocity unique to the interface region difficult.

If the transition between the jet and the ambient medium can be resolved, we might expect relatively large differences between the profiles of charged and neutral species. The ion flow would be laminar, and would show a smooth transition between the velocity of the core of the jet and the velocity of the ambient medium. The neutral flow would show the

same range of velocities, but would be turbulent, leading to broader lines.

## 4.2. Heating

Figure 4 predict that throughout most of parameter space, the magnetic field prevents the ions from participating in unstable perturbations. The resulting velocity difference between the ions and neutrals creates friction that can heat the gas. The heating rate per unit volume is given by

$$\Gamma_{fric} = \rho_n \nu_{ni} (v_n - v_i)^2 \approx \rho_n \nu_{ni} v_n^2. \quad (37)$$

For example, assuming  $v_n \sim 1 \text{ km s}^{-1}$ ,  $n_n = 10^3 \text{ cm}^{-3}$ ,  $n_i = 10^{-4} \text{ cm}^{-3}$  gives  $\Gamma_{fric} \sim 6 \times 10^{-24} \text{ ergs cm}^{-3} \text{ s}^{-1}$ . Assuming that the heating is balanced by radiative cooling, the corresponding luminosity density is  $0.04 L_\odot \text{ pc}^{-3}$ . The frictional heating rate dominates cosmic ray heating. Taking the latter from Spitzer (1978) we find

$$\frac{\Gamma_{fric}}{\Gamma_{CR}} = 1.5 \times 10^6 n_i v_5^2, \quad (38)$$

where  $v_5$  is the neutral velocity in km/s. Unlike viscous heating, which is also strong in a turbulent boundary layer,  $\Gamma_{fric}$  is independent of the thickness of the layer.

## 4.3. Magnetic field configuration

The orientation of the magnetic field in the outflow could be mapped by measuring the polarization of infrared radiation emitted by the dust grains. According to our analysis, the magnetic field should remain well organized even though the neutral flow is turbulent, provided that the mean field is aligned with the flow (if the field were transverse to the flow, the plasma would be unstable, and would carry the field with it, but the turbulent motions would be perpendicular to the field, and would not strongly bend it).

Observations of a turbulent field in the outflow could be explained if the ionization fraction were much larger than assumed here, resulting in stronger coupling, or if the grains were aligned by the turbulent neutral flow rather than by the magnetic field. Observations of a straight field, however, demonstrate only that the field is well organized at or above the scale resolved by the observations (Heitsch et al. 2001). A low polarized intensity could be evidence for a disordered field below the resolved scale, but could also be due to poor alignment of the grains (Padoan et al. 2001).

## 5. Conclusions

Outflows from massive protostars are observed to carry a large mass flux and to be poorly collimated. Both properties suggest that these outflows entrain substantial volumes of ambient ISM material. Turbulence driven by shear flow instabilities at the interface between the jet and the surrounding medium is one possible mechanism for entrainment.

In this paper we have examined the Kelvin-Helmholtz instability in a weakly ionized medium with parameters chosen to be similar to molecular outflows. In order to study effects introduced by two fluids (plasma and neutral), we chose the simplest possible geometry: two uniform media (taken in all examples to have the same density) in relative motion at speed  $U$ , separated by a sharp interface, with a uniform magnetic field parallel to the flow. Under these conditions, a plasma is unstable if the relative velocity exceeds the Alfvén speed (Chandrasekhar 1961). For the parameters of interest to our problem, the plasma is magnetically stabilized while the neutrals, in the absence of frictional coupling to the ions, would always be unstable. In the limit of perfect frictional coupling, the combined system - with the Alfvén speed based on the total mass density instead of the plasma density - could be either stable or unstable, according to whether the bulk Alfvén speed  $v_A$  exceeds  $U$ .

Most of the analysis in our paper is based on the dispersion relation derived in §2, equation (30). Our main result is that for much of the size range of interest, the ions and neutrals are sufficiently decoupled that the neutrals are unstable, while the ions are held in place by the magnetic field. At short scales, the growth rate is well approximated by the growth rate of the hydrodynamic instability,  $kU$ . At longer scales, the fastest growing mode is either the magnetically modified MHD mode, if the magnetic field is weak enough ( $v_A < U$ ), or, if  $v_A > U$ , a new mode with growth rate  $kU(kU/\nu)$ . The transition between these modes of instability occurs at  $kU/\nu \approx 1$ . The dispersion diagram is plotted in Figure 2. The relative amplitudes of the ion and neutral fluctuations are shown in Figure 4, demonstrating that over most of the regime of interest, the ions drop out of the instability.

We believe these results continue to hold in cylindrical geometry. In fact, they should be even more pronounced because at short wavelengths the cylindrical and planar cases coincide, while at long wavelengths the instability is suppressed by geometry. We also expect that more general perturbations, such as those with a large transverse wavenumber  $k_y$ , would be characterized by similar ion-neutral decoupling.

Although we have not followed the instability into the nonlinear stage, there is no reason why frictional coupling should be more efficient at large amplitude, so we expect our results to apply to the nonlinear regime. There is, however, a compelling case to be made for nonlinear calculations: they are necessary to produce detailed observational predictions. As

such, they should follow the thermal and chemical state of the gas, as well as its dynamics.

Based on the linear theory, however, it appears that our model may be tested in several ways, mentioned in §4; differences in line profiles between charged and neutral species, efficient heating by ion-neutral friction, and the polarimetric signature of a well organized magnetic field. We will report on spectroscopic evidence in a forthcoming paper (Watson et al. 2004).

Our results do, however, leave us with a conundrum. Churchwell (1997) pointed out that the rate of entrainment required to explain the mass flux in outflows is unreasonably large, if the entrainment is hydrodynamic in nature. The low degree of ion-neutral coupling predicted by our model suggests that the entrainment is more hydrodynamic than magnetohydrodynamic, although nonlinear simulations and analysis are necessary to settle the issue.

We are happy to acknowledge support by NSF grant AST-0328821, NSF PHY-0215581 and by the Graduate School of the University of Wisconsin, Madison. F.H. is grateful for support by a Feodor-Lynen Fellowship from the Alexander von Humboldt Foundation.

### A. Ions Held Stationary

We begin with the same assumptions as specified in section 2, with the additional assumption that the ions remain at rest. That is, they are not disturbed by the perturbation. The equation of motion for the neutral particles is:

$$\rho_n \partial_t \mathbf{v}_n + \rho_n \mathbf{v}_n \cdot \nabla \mathbf{v}_n = -\nabla P_n - \rho_n \nu_{ni} \mathbf{v}_n \quad (\text{A1})$$

Assuming a periodic perturbation, we obtain:

$$\rho_n (\omega + Uk_x) u_n = -k_x P_n + i \rho_n \nu u_n \quad (\text{A2})$$

$$\rho_n (\omega + Uk_x) w_n = i \partial_z P_n + i \rho_n \nu w_n. \quad (\text{A3})$$

Taking the curl and combining to eliminate the pressure term, we obtain

$$\rho_n (\omega + Uk_x - i\nu) (\partial_z^2 - k_x^2) w_n = 0 \quad (\text{A4})$$

We integrate over the interface to obtain,

$$\Delta \{ \rho_n (\omega + Uk) \partial_z w_n \} = i \Delta \{ \rho_n \nu \partial_z w_n \} \quad (\text{A5})$$

We introduce a solution of the form

$$w_{n1} = \mathcal{A}(\omega + Uk)e^{kz} \quad z < 0 \quad (\text{A6})$$

$$w_{n2} = \mathcal{A}(\omega + Uk)e^{-kz} \quad z > 0 \quad (\text{A7})$$

to obtain

$$\rho_n(\omega + Uk)^2 - i\rho_n\nu(\omega - Uk) = 0 \quad (\text{A8})$$

After converting to dimensionless notation, we obtain

$$x^2 + h^2 - ix = 0 \quad (\text{A9})$$

$$x = \frac{1}{2} \left( i \pm \sqrt{-1 - 4h^2} \right) \quad (\text{A10})$$

$$x \approx \frac{1}{2} \left( i \pm i(1 + 2h^2) \right) \quad (\text{A11})$$

For  $h \ll 1$ ,

$$x \approx i, -ih^2. \quad (\text{A12})$$

Thus, we see that the  $-ih^2$  mode observed in section 2 originates from the uniform drag that the neutral particles feel from the uniformly distributed ionized particles.

## REFERENCES

Bachiller, R. & Tafalla, M. 1999, NATO ASIC Proc. 540: The Origin of Stars and Planetary Systems, 227

Table 1. Unstable Roots of Characteristic Equation

$x^4 - imx^3 - a^2x^2 - i(mh^2 - a^2)x - a^2h^2 = 0$						
(1)	(2)	(3)	(4)	(5)	(6)	
Root	Dominant Terms		Physical Regime			
$-ih$	3, 6		$h > 1$			
$-ih^2$	5, 6		$1 > h$ and $\frac{a}{\sqrt{m}} > h$			
$i(\frac{1}{2} \pm h)$	3, 4, 5, 6		$\frac{a}{\sqrt{m}} > h > 1$			

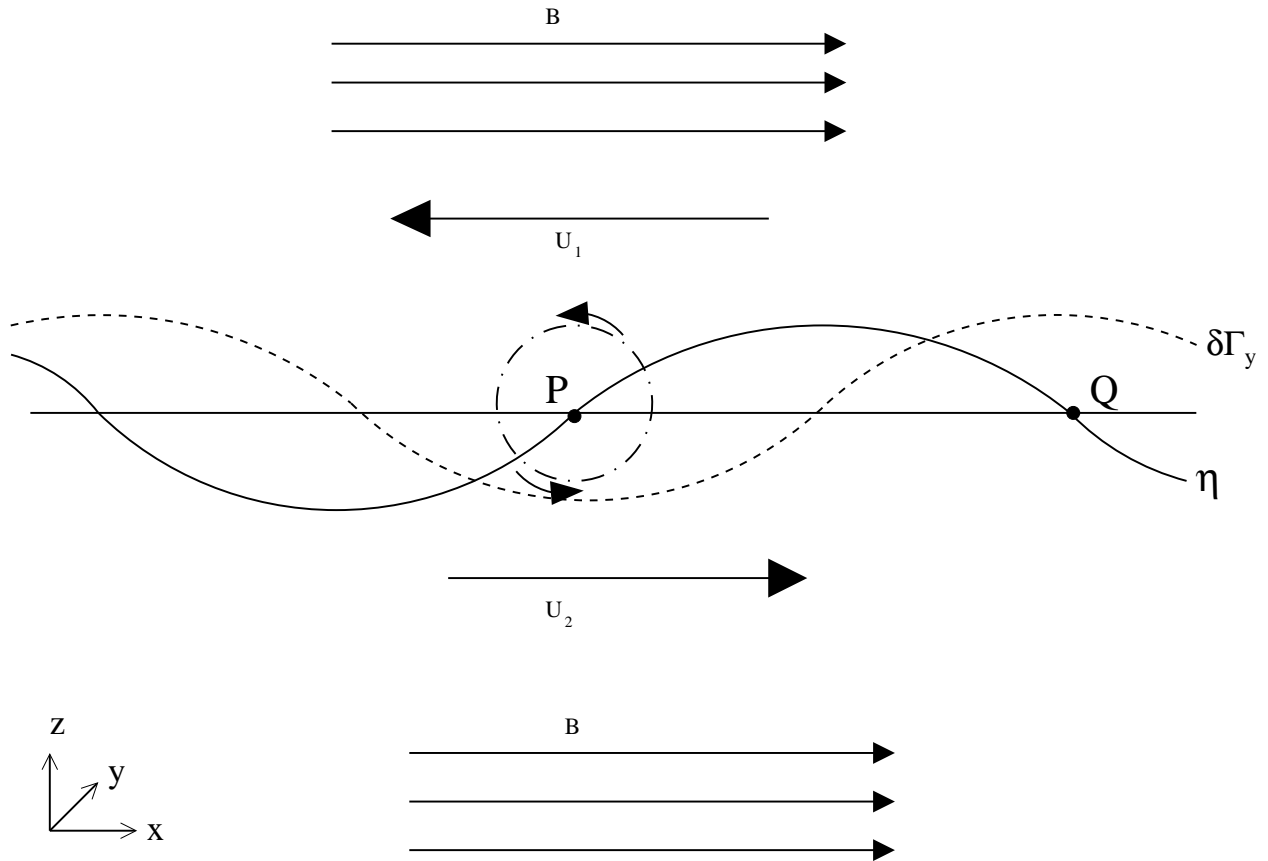


Fig. 1.— Diagram of the standard Kelvin-Helmholtz instability. Since the fluid is assumed to be incompressible, a small periodic perturbation at a shear layer will tend to grow. In general, the vorticity perturbation ( $\delta\Gamma_y$ ) is out of phase with the vertical displacement of the vortex sheet ( $\eta$ ). If it can be arranged that the vorticity has the distribution shown by the dashed line, then the equilibrium flow sweeps negative vorticity toward point  $P$ . The effect is as if an “extra eddy”, rotating counterclockwise were added to the flow. The centrifugal force associated with the eddy pushes the interface between  $P$  and  $Q$  outward, resulting in the growth of  $\eta$  with time.



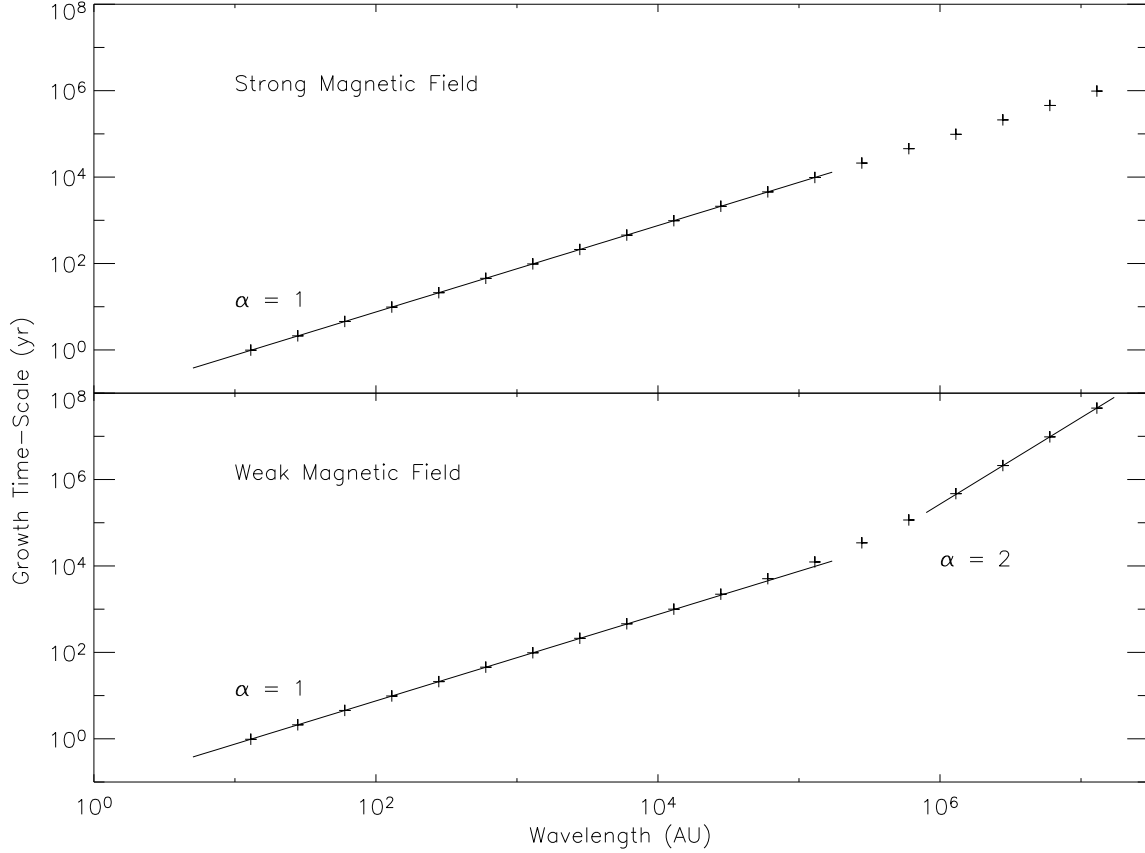


Fig. 2.— The growing instability root of the characteristic equation as a function of wavelength. The strong magnetic field regime (top) assumes  $U = 10 \text{ km s}^{-1}$  and  $B = 1 \text{ mG}$  and the weak magnetic field regime (bottom) assumes  $U = 10 \text{ km s}^{-1}$  and  $B = 1 \mu\text{G}$ . The crosses represents the numerically determined root. The solid lines represent the analytic approximation to root,  $h$  ( $h$ ) at short wavelengths and  $h$  ( $h^2$ ) at long wavelengths for the strong (weak) magnetic field regime.

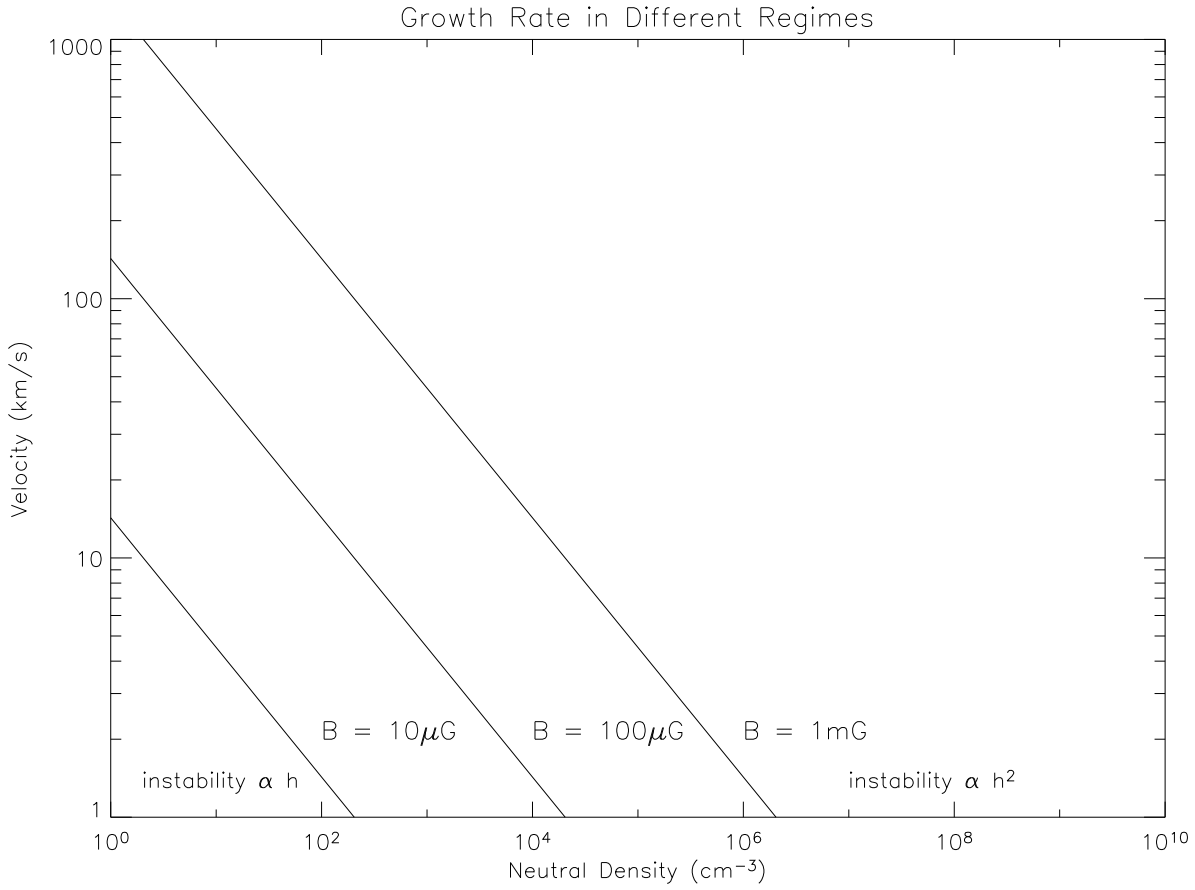


Fig. 3.— The growth rate of the Kelvin-Helmholtz instability depends on the density, flow velocity and magnetic field strength. The transition between the standard Kelvin-Helmholtz instability (growth rate  $\propto h$ ) and the new, slower instability (growth rate  $\propto h^2$ ) is given for 3 magnetic field strengths.

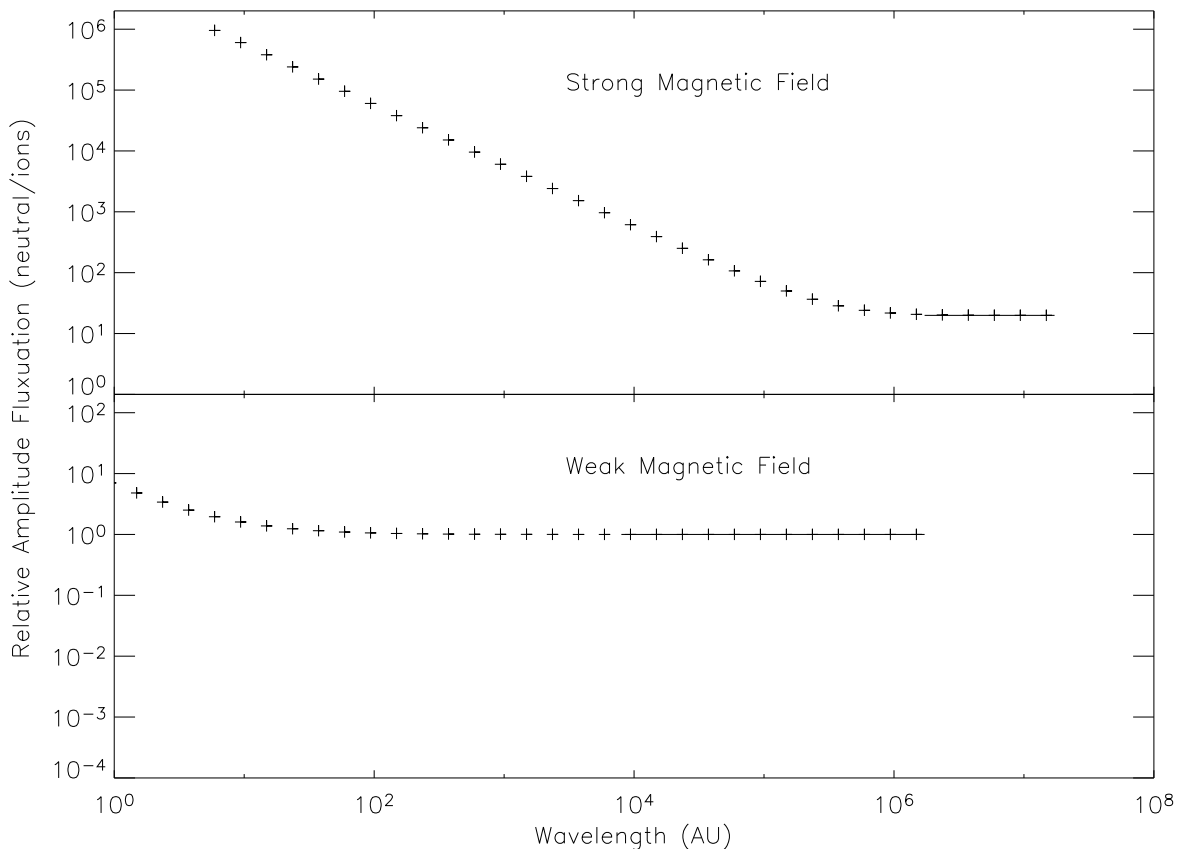


Fig. 4.— The amplitude of the neutral perturbations relative to the ion perturbations. Numerical results are represented by crosses. The lines represents the analytic approximations to the relative perturbations as specified above. The strong magnetic field regime (top) assumes  $U = 10 \text{ km s}^{-1}$  and  $B = 1 \text{ mG}$  and the weak magnetic field regime (bottom) assumes  $U = 10 \text{ km s}^{-1}$  and  $B = 1 \text{ } \mu\text{G}$ .

- Batchelor, G.K. 1967, *An Introduction to Fluid Dynamics*, Cambridge University Press
- Chandrasekhar, S. 1961, *Hydrodynamic and Hydromagnetic Stability*, Oxford University Press
- Churchwell, E. 1997, ApJ, 479, L59
- Drazin, P. G. & Reid, W. H. 1981, *Hydrodynamic Stability*, Cambridge Univ. Press
- Heitsch, F., Zweibel, E.G., Mac Low, M-M., Li, P., & Norman, M.L. 2001, ApJ, 561, 800
- Hughes, D.W., & Tobias, S.M. 2001, Proc. Roy. Soc. Lond. A., 457, 1365
- Jones, T. W., Gaalaas, J. B., Ryu, D., & Frank, A. 1997, ApJ, 482, 230
- Kulsrud, R. & Pearce, W. P. 1969, ApJ, 156, 445
- Malagoli, A., Bodo, G., & Rosner, R. 1996, ApJ, 456, 708
- Padoan, P., Goodman, A., Draine, B.T., Juvela, M., Nordlund, A., & Rögnerdsson, Ö.E. 2001, ApJ, 559, 1005
- Spitzer, L. 1978, *Physical Processes in the Interstellar Medium* (New York: Wiley-Interscience)
- Watson, C., Churchwell, E., Zweibel, E.G., Crutcher, R. 2004, in prep.
- Wolfram, S. 1999, *The Mathematica Book* (4th ed.; Champaign/New York: Wolfram Media/Cambridge Univ. Press)